Component Development for a 10-cm Mercury Ion Thruster

J. W. PYE*
Royal Aircraft Establishment, Farnborough, Hampshire, England

Three feed system components are described, namely a high-voltage isolator, a liquid mercury flowmeter, and a porous tunsten vaporizer. An experimental investigation of a simple lightweight isolator incorporating an insulating porous core to assist charge recombination resulted in the attainment of standoff voltages of 7.5 kv with leakage currents below 10 μa. A promising flowmeter utilizing a thermal principle was shown to have a sensitivity of 0.8 mv (mg/sec)$^{-1}$ with good linearity. A small efficient vaporizer having a typical power dissipation of under 1.5 w at 0.5 mg sec^{-1} is described. Wherever possible, reference is made to calibration technique and the relevant theory.

Introduction

A BROAD range of component development, a part of which has already been reported in some detail,[1,2] is in progress at the RAE in support of a 10-cm mercury ion thruster using a hollow cathode electron source.[3] This paper presents the designs and describes the performance characteristics of the three major components developed for use in a pressurized mercury feed system. As the empirical approach to ion thruster investigations, although eventually effective, is not thought to be economical of manpower or resources, an attempt has been made throughout this work to obtain a clear understanding of the physical principles involved in the operation of each component. This should enable future designs to be produced with confidence and will also allow assessments of the advantages of further development.

High-Voltage, High-Pressure Isolator

The operational advantages of using an isolation device for electrically separating the ion thruster from the mercury propellant feed system have been discussed many times and need not be elaborated here. Although a plain tubular ceramic isolator may suffice for the propellant flow to the discharge chamber[4] and has been successfully used for this purpose in the RAE,[5] the high pressure in the independently controlled cathode feed path (0–50 torr) complicates the design of the other isolator. Consequently, experiments have been conducted to investigate the effectiveness of internal porous insulating media to promote surface recombination of ions and electrons and thus inhibit high pressure breakdown. Another principle, that of providing a long flow path to ensure that operation is always on the right-hand limb of the Paschen curve for mercury vapor, was also investigated. In both cases, very satisfactory results were obtained, although the porous structure isolator described here appeared to possess greater advantages.

Investigation of Porous Media Isolators

The principal object of this investigation was to determine the effect of porous insulating media on the breakdown voltage and leakage current of a tubular ceramic isolator within an appropriate range of pressures. Different materials and dimensions were also studied.

Initially, lead glass spheres were used to simulate a porous structure because they were readily available in a range of convenient sizes and the material offered desirable electrical properties.[6] This isolator, shown in Fig. 1a, consisted of a 5 mm i.d., 6-cm-long alumina tube filled with the spheres under test, which were held under compression by springs. One end of the tube was either blanked off or connected to a hollow cathode discharge system, whereas a vaporizer,[2] controlling the vapor pressure or mass flow, was connected to the other. All components were heated to a temperature above that of the vaporizer to avoid mercury condensation, the isolator being maintained at a uniform 280°C. The centrally positioned heater winding was usually earthed to avoid inconsistencies due to variable surface leakage currents.

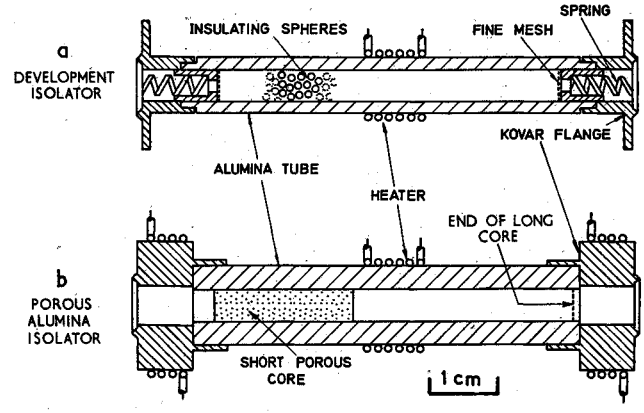

Fig. 1 Constructional details of isolators.

As a logical conclusion to the development phase of the program, an isolator was manufactured by sintering porous alumina cores, formed from spheres of known dimensions, into tubes of the same material, as shown in Fig. 1b. For purposes of performance comparisons, the internal dimensions of the tube were identical to those employed previously. However, because of the high radial stresses involved in the sintering process, a wall thickness of 3 mm was necessary, resulting in a more bulky design. Two variations of the internal structure were investigated. The first was a core formed from 1.6–2.0-mm-diam alumina spheres and occupying the full length of the tube, and the second was a 2-cm-long core, situated at the thruster end, formed from 0.75–0.9-mm-diam alumina spheres.

Test Apparatus and Procedure

In all experiments, breakdown characteristics were obtained with either mercury vapor pressure P_v or mass flow rate $\dot{m}$ as the controlling variable, an operating hollow cathode being attached to the isolator under test in the latter case. Correlation of the two sets of data for a given isolator allowed estimates to be made of P_v as a function of $\dot{m}$.

A schematic of the test apparatus is shown in Fig. 2. For those tests giving breakdown voltage V_B as a function of P_v, a

Presented as Paper 72-487 at the AIAA 9th Electric Propulsion Conference, Bethesda, Md., April 17–19, 1972; submitted April 4, 1972; revision received October 3, 1972. British Crown Copyright reproduced with permission of the Controller, Her Britannic Majesty's Stationery Office. The author wishes to thank D. G. Fearn for advice and many fruitful discussions throughout the course of this work.

Index category: Electric and Advanced Space Propulsion.

* Higher Scientific Officer, Space Department.

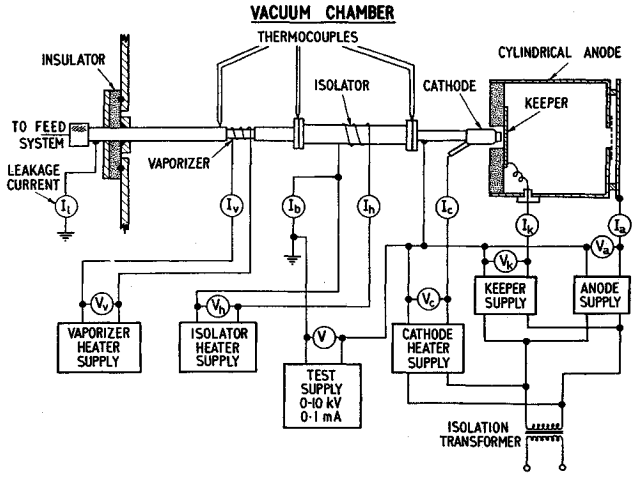

Fig. 2 Schematic of isolator test apparatus.

heated blanking-off cap was substituted for the hollow cathode assembly. Seals in the vapor feed system consisted of thin nickel gaskets compressed against flat surfaces by knife edges. Values of P_v were established by setting the vaporizer temperature, as indicated by the surface thermocouple (see final section), to the appropriate value. This value was related to the porous plug temperature, and hence P_v, by a previous calibration. When a hollow cathode was used, $\dot{m}$ was evaluated from the rate of fall of the mercury meniscus in a precision bore glass capillary reservoir. A subsidiary vacuum line was provided to allow for initial evacuation of the isolator under test.

A cylindrical anode was used to contain the hollow cathode discharge plasma and prevent leakage currents from reaching the surrounding vacuum chamber walls. The latter feature allowed a high voltage source of limited current capability to be used, thus preventing possible destructive breakdown of the isolator under test. Tests were conducted in a 0.35 m diam, 0.46 m-long vacuum chamber containing a liquid nitrogen cooled shroud. The pressure was maintained at 10^{-5} to 10^{-4} torr (depending on mercury vapor flow rate) by a 15 cm mercury diffusion pump.

Results from Studies of Porous Structure Isolators

Figure 3 shows V_B as a function of P_v for a range of glass sphere sizes and for the empty tube. From these results, it was clear that the breakdown characteristics were considerably improved by the presence of such spheres as, at any pressure, V_B increased rapidly with decrease in sphere size. The concept of using a large surface area to encourage recombination was thus validated. At high pressures, all experimental curves became asymptotic to that for the empty tube. Breakdown was nearly always characterised by a sudden large increase in current from a negligibly small value (<10 μa). An exception was a transition to a low current luminous discharge in the empty tube, in which case breakdown was arbitrarily defined as the attainment of a current of 100 μa.

The results obtained using isolators incorporating alumina cores were very similar to those just described. Consequently, there was little difference between these materials and techniques, suggesting that geometry and surface area presented to the vapor flow were the dominant parameters. In general, therefore, the breakdown curves for all isolators containing porous media exhibited Paschen-type characteristics, with the minimum value of V_B and corresponding values of P_v being functions of sphere diameter d. For clarity, these parameters have been compared in Fig. 4.

From a study of these results, several important facts emerge. First, as already mentioned, there appears to be little difference between lead glass and alumina when comparing minimum breakdown voltage $V_{B\,\min}$ and the corresponding P_v for a given sphere size. However, geometry is very important, as was shown when it was attempted to obtain a very high internal surface area by filling an isolator with hollow alumina cylinders. The breakdown characteristics of this arrangement were only marginally better than those of an empty tube, due to the fortuitous provision of an almost direct breakdown path through the packed cylinders.

For either material, V_B was little affected when the length of the porous insert was considerably reduced. This was first demonstrated by the use of an internal electrode extension in the isolator, shown in Fig. 1a, to effectively reduce the length of the porous medium. It was later confirmed by tests of the sintered alumina devices (Fig. 4). This result is difficult to explain solely by consideration of charge recombination following diffusion to the internal surfaces, and is more likely to be the result of an uneven distribution of space charges within the isolator, which gives locally high electric fields at or near the electrodes. Since these fields would be dominant in accelerating particles to high energy and thus initiating breakdown, the tube length could be varied over quite wide limits before significantly affecting V_B. The existence of these fields was confirmed by inserting small probes into the porous medium, and by experiments in which the breakdown characteristics were significantly modified by imposing particular field configurations by external means.

Figure 4 shows that, within the limits of the experiment, the values of P_v at $V_{B\,\min}$ were inversely proportional to d, closely following the curve $P_v = 15/d$. This relationship between P_v and d (or void dimension) can be explained by reference to the Paschen Law, and is consistent with the initiation of discharges within the voids in the region of

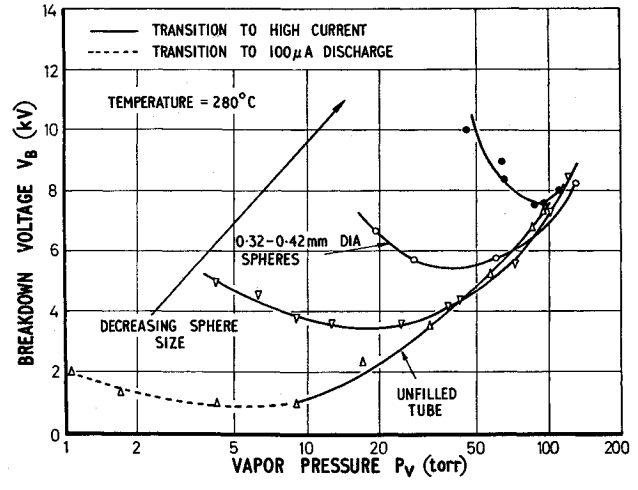

Fig. 3 Breakdown voltage as a function of vapor pressure for a range of glass sphere sizes.

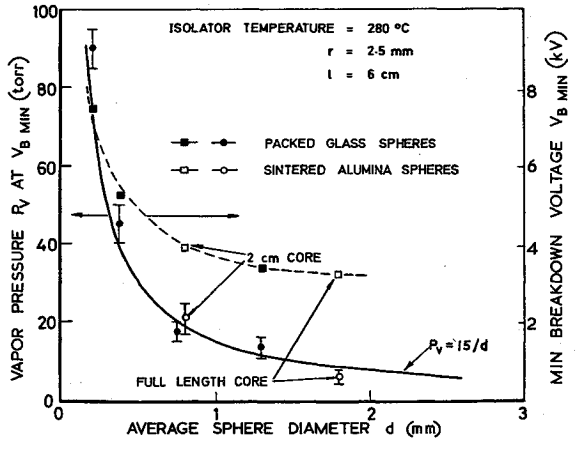

Fig. 4 Vapor pressure at the minimum breakdown voltage and minimum breakdown voltage as functions of sphere diameter.

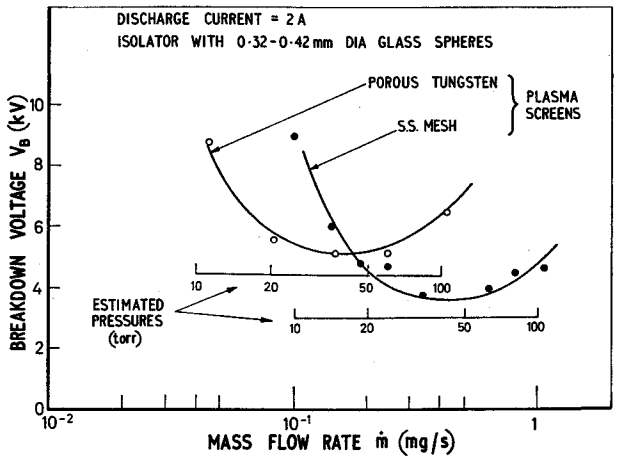

Fig. 5 Isolator breakdown characteristics when operating with a hollow cathode.

maximum electric field.[7] The Paschen curve for mercury vapor is dependent both on electrode geometry[8,9] and material.[10] At the minimum, $P_0\delta = R$, where P_0 is the pressure referred to 0°C, δ is the electrode separation, and R is a constant, usually in the range 0.5–2.0 torr-cm, which is dependent on geometry and materials. In the present case, the maximum electric field and initial breakdown sites were probably adjacent to the cathode. Thus a value of R intermediate between that for nickel[10] (0.5 torr-cm) and for steel[8] (1.1 torr-cm) would seem appropriate. Taking $R = 0.8$ torr-cm, d to be a measure of the dimensions of a typical void, and evaluating P_0 from $P_0 = 273P_v/(T + 273)$, where T is the isolator temperature in degrees C, $P_v = 16/d$ if d is in millimeters. This is very close to the experimentally determined relationship between P_v and d. It may therefore be postulated that the initial breakdown occurs across a single void in the high-field region. This void is then unable to sustain the electric field, and the potential across the next void is correspondingly increased. This then breaks down, the ionized gas in the first acting as a virtual cathode, and the process continues rapidly.

Tests with Hollow Cathode

It is evident from the experiments described above that any diffusion of plasma from a hollow cathode into an isolator could initiate the breakdown process. Photoemission caused by UV radiation could have a similar effect. Consequently tests were made with various plasma containment screens situated between an isolator and a hollow cathode[1] operating at a discharge current of 2 amp.

The results illustrated in Fig. 5 were obtained using a cylindrical porous tungsten plug (see section on vaporizers) and a wire mesh as containment screens. It is evident, from a comparison with Fig. 3, that both $V_{B\min}$ and the general shape of the breakdown characteristic were unaffected by the cathode when using the porous tungsten plug. In contrast, the use of a fine stainless steel mesh with an average aperture of 0.15 mm resulted in a lowering of $V_{B\min}$ from 5 kv to 3.5 kv. The performance deteriorated further when no screen was employed.

Correlation of the data for a given isolator operated with and without a hollow cathode allowed estimates to be made of P_v as a function of $\dot{m}$. These values are shown in Fig. 5. It is also interesting to note that the values of P_v with the stainless-steel mesh plasma screen inserted would be expected to bear a close relationship to the hollow cathode pressure, confirming typical operating pressures of 10–20 torr.[11]

Liquid Mercury Flowmeter

The accurate and continuous measurement of propellant mass flow rate is considered to be essential in the long term as a control parameter in ion thruster systems. This will allow the propellant utilization efficiency to be maintained constant, as may be required in certain missions, or will enable an optimum compromise to be reached between high values of this parameter and of the power efficiency. It is not possible to rely on the flow rate-temperature calibration of the vaporizer owing to the possibility of partial blockage or progressive wetting of the porous tungsten plug over long periods. In this connection, a thermal flowmeter is described which has a sensitivity of 0.8 mv $(\text{mg/sec})^{-1}$ with good linearity.

Operating Principle

The flowmeter design was based on a thermal principle,[12] and consisted of a propellant flow tube heated at its center, with the ends terminating in constant-temperature heat sinks. The temperature gradient along the tube was strongly dependent on the rate of flow of liquid through it. Thus a differential temperature measurement could, by suitable calibration, be related to the flow rate.

Experimental Model

The relevant constructional details of the experimental model are shown in Fig. 6. A stainless steel flow tube 6 cm long and 1 mm i.d., with a 0.0125-mm wall thickness, had its ends held in good thermal contact with the molybdenum heat sink forming the body of the instrument. The heater consisted of 6 turns of 0.5-mm-diam stainless-steel sheathed heating cable, vacuum brazed to the center of the tube. A temperature controller maintained the temperature difference between the heater and body constant with an accuracy of better than 1%. A system of closely positioned tantalum foil radiation shields was included to minimize power dissipation and distortion of the axial temperature profile caused by radial heat flow. Teflon supports were used to reduce conduction losses, both between the shields and to the body.

With no flow through the tube, the temperatures measured at positions midway between the heat source and heat sink, shown as points E and F in Fig. 6, were approximately equal. Any flow, however, caused the upstream point to be cooled, while the downstream one was heated by mercury coming from the vicinity of the heater. A temperature difference was therefore set up, which could be related to flow rate by use of

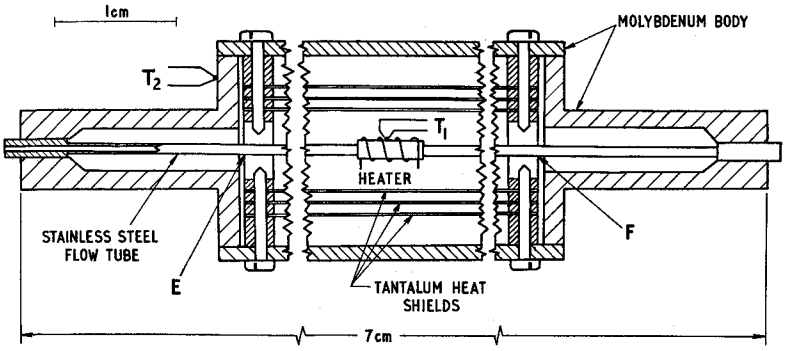

Fig. 6 Experimental flowmeter.

a previous calibration employing the glass capillary tube system mentioned earlier.

The temperature measurements were obtained using a differential thermojunction system which utilized the stainless steel flow tube as the common element, with thin constantan wires spot welded to the tube at E and F to form the dissimilar metal junctions. A calibration of this combination yielded a sensitivity of 45 μv $C^{\circ -1}$ over the operating temperature range.

Method of Calibration

The flowmeter was calibrated by measuring the thermojunction output voltage V_T as a function of flow rate, which was controlled by a specially designed mercury vaporizer. The latter was of a type discussed in the final section but with an exceptionally small heated volume of mercury. Thus errors due to expansion and contraction of this volume (thermometer effect) following adjustments to the vaporizer temperature were minimized. The vaporizer-flowmeter assembly was mounted on the vacuum chamber access flange which also served as a convenient heat sink for the vaporizer. A 1-mm-diam, 10-cm-long feed tube, linking the two components, provided thermal decoupling.

Results and Discussion

The experimentally determined thermojunction output voltages and corresponding differential temperature changes ΔT are shown as functions of mass flow rate in Fig. 7 for three heater temperatures T_1, the body temperature T_2 being held constant at 50°C. These results followed a substantially linear relationship with a small offset voltage at zero flow rate which changed at the lower value of T_1 only. Although this nonzero output can be explained in terms of a small discrepancy in the relative axial positions of the two thermojunctions, this does not account for its reduction to almost zero for $T_1 = 200$°C. Another factor which may have contributed to this effect was the use of an epoxy resin as a bonding agent between the flow tube and heat sink, causing inadequate thermal coupling. It is hoped that this problem can be overcome in a later version by using a vacuum brazing process together with more accurate alignment of the thermojunctions.

It is apparent from Fig. 7 that the sensitivity of the instrument was a function of $(T_1 - T_2)$, as expected from the theory presented below. In terms of ΔT, there was clearly a high sensitivity, which was measured to be 18°C $(mg/sec)^{-1}$. Unfortunately, this was not fully realizable, owing to the relatively small output of thermoelectric devices, and the highest value recorded was 0.8 mv $(mg/sec)^{-1}$. The use of thermistors to sense the temperature difference would result in a very substantial improvement. This was shown to be the case in a very recent publication by Wilbur,[13] who described a similar instrument with an estimated sensitivity of 24 mv $(mg/sec)^{-1}$.

To maintain the liquid in a stable state in the vicinity of both the flowmeter and vaporizer heaters, it was considered necessary to restrict T_1 to below 300°C. This limited the sensitivity to the above value. At that temperature, the power dissipation was less than 1 w.

A precise estimate of the repeatability of the measurements was limited by the calibration errors. Despite this, the over-all consistency was better than 2%, as indicated by the error bars in Fig. 7, which is largely attributed to the small liquid capacity and relatively short thermal time constant of the vaporizer. As a measure of the combined transient performance, V_T required about 120 sec to stabilize for a vaporizer temperature change of 300°C–210°C, in response to a step change in vaporizer heater current.

Correlation of Experiment with Theory

By assuming that radial heat losses by conduction and radiation were negligible and that the fluid velocity v was uniform over the tube cross section, it was possible to theoretically derive an expression for the temperature distribution along the flow tube.[14] If the temperature at distance x from the edge of the heated region is T,

$$T = [T_1(e^{AL}e^{-Ax} - 1) - T_2e^{AL}(e^{-Ax} - 1)]/(e^{AL} - 1) \quad (1)$$

where L is the effective length of the flow tube from heat source to heat sink and $A = (\rho cv/K)$, where K, c, and ρ are the thermal conductivity, specific heat, and density of liquid mercury, respectively. Also x, L, and v may have both positive and negative values, depending on which symmetrical half of the flow tube is considered. A multiplying factor should be included in Eq. (1) to allow for the thermal shunting caused by the flow tube wall. This is

$$\{1 + (K_1/K)(D^2 - d^2)/d^2\}^{-1}$$

where K_1, D, and d are the thermal conductivity and the external and internal diameters of the flow tube, respectively.

From Eq. (1) it was possible to estimate the temperature difference ΔT between points E and F in Fig. 6 as a function of A, and thus of v. These theoretical results are compared with the experimental data in Fig. 8, for both the ideal case and for that in which the tube wall causes thermal shunting. It is evident that the ideal theoretical sensitivity was appreciably higher than that found experimentally, but the thermal shunting effect of the flow tube wall reduced this discrepancy to less than 20%. The remaining difference may be accounted for by including the residual radial heat flow and, possibly to a lesser extent, by the fluid velocity profile.

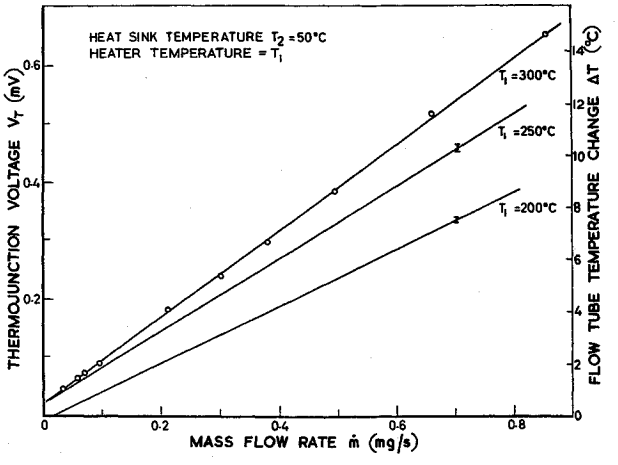

Fig. 7 Flowmeter thermojunction voltage and corresponding differential temperature change as functions of mass flow rate.

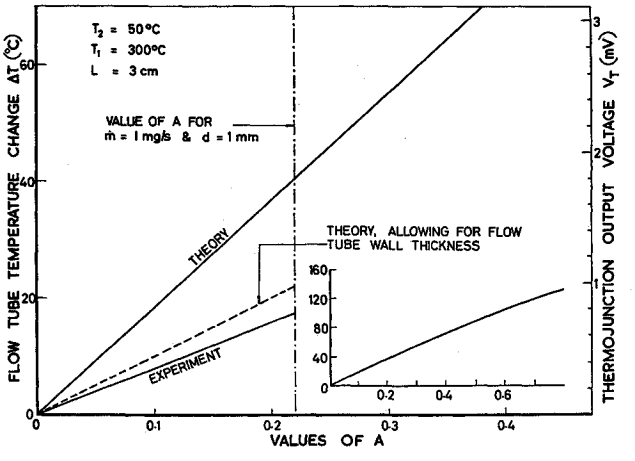

Fig. 8 Comparison of experimental with theoretical results for the flowmeter.

It is evident from Fig. 8 that, with the present thermojunction arrangement, an increase in sensitivity of at least a factor of four should be practicable, while retaining good linearity, by further reductions in both d and the tube wall thickness. If this is still inadequate for certain applications, a different method of sensing ΔT can be employed to yield a larger output signal.[13]

Vaporizers

A development program providing the information required to design an efficient reliable mercury vaporizer, which employs the usual heated porous tungsten plug as a liquid/vapor phase separator, has been reported earlier.[2] Similar work carried out independently has recently been described by both Kerslake[15] and Arlt.[16] A summary of the important results mentioned in Ref. 2 is given here, together with a discussion of additional progress made more recently. The eventual aim of the work is to design vaporizers for the three different mass flow requirements. For example, in a thruster giving a beam current of 250 ma, a total flow rate of about 0.6 mg sec^{-1} is needed, of which 10–30% passes through the hollow cathode and 1–2% through the neutralizer.[17]

Design Concept and Construction

Initial vaporizer development involved a basic tubular configuration, which was amenable to miniaturization and simple to construct. This is shown in Fig. 9. To vary the vapor mass flow rate $\dot{m}$ over a wide range at reasonable operating temperatures, two types of vaporizer were produced with tungsten plugs of different effective areas. For the low flows, a simple disk shape was used, while higher flows were more economically achieved with a cross section having greatly increased area. A theoretical relationship between $\dot{m}$ and the various plug parameters was developed and is summarized below.

The porous plug was welded into a 5-mm-o.d. molybdenum tube, this material being chosen for its high thermal conductivity and welding compatibility with tungsten. The heating element was attached to the outside surface of the tube, and stainless-steel pipes were welded to its ends. Two types of heater were used. A nichrome tape encased in flame-sprayed alumina was reliable and effective for laboratory testing, while a stainless-steel sheathed heating cable brazed onto the molybdenum tube was considered perhaps more suitable for flight application.

Vaporizer Performance

Experiments were performed using the vacuum chamber and flow monitoring apparatus discussed previously. As shown in Fig. 10, flow rates exceeding 1 mg sec^{-1} were readily attainable at moderate temperatures, and, at a given temperature, $\dot{m}$ was increased very effectively by using a plug of larger area but the same porosity. Moreover, as illustrated in Fig. 11, an increase in plug area also caused a significant reduction in the power required to give a particular flow rate, as did the use of smaller-diameter liquid and vapor feed tubes and brazed-on heaters. For example, for a flow rate of 0.5 mg sec^{-1}, the power input required with a disc plug was reduced from 6.8 to 1.7 w by using narrow feed tubes and a brazed-on heater, with a further reduction to 1.2 w when a large-area plug was employed. The liquid pressure used in these experiments was 1.5 atm. Reducing this to 0.5 atm caused the flow rate at a given temperature to decrease by approximately 25%, possibly due to a decreased depth of penetration of the mercury meniscus into the porous structure. An experimental investigation of this effect at higher liquid pressures has been reported by Bessling.[18]

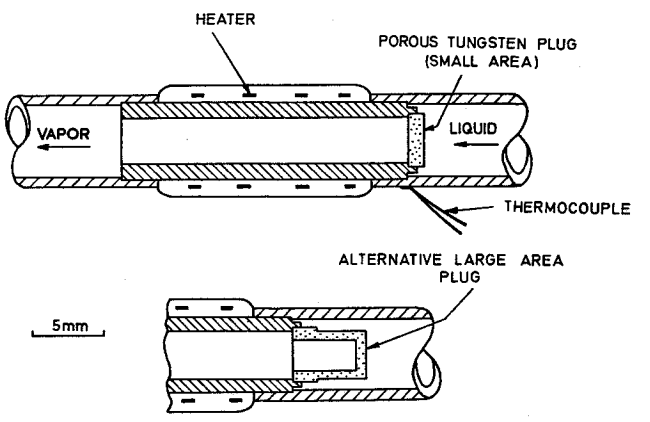

Fig. 9 Basic tubular vaporizer configurations.

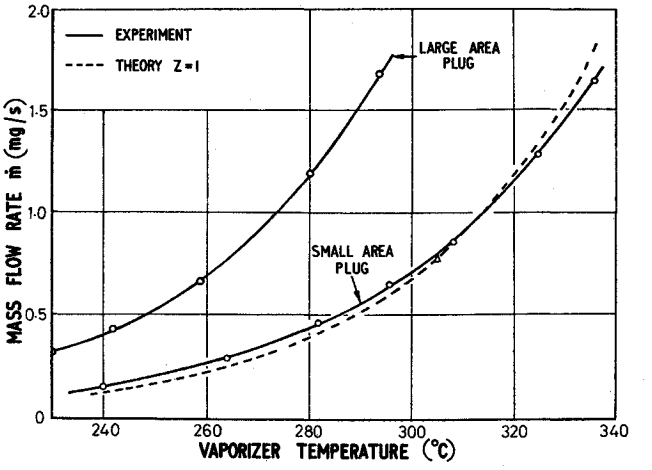

Fig. 10 Vaporizer flow rate as a function of temperature.

Tests with Ion Thrusters

Vaporizers of the type discussed have now been operated with an ion thruster for over 1500 hr with complete reliability. In separate life test experiments, a time equivalent of 2000 hr at a bypass flow rate of 0.5 mg sec^{-1} or 10000 hr at a cathode flow rate of 0.1 mg sec^{-1} has been achieved with no obvious sign of degradation. These tests involved no special precautions other than using triple distilled and outgassed mercury.

Problems due to variations in discharge current causing changes in internal hollow cathode pressure and hence $\dot{m}$ were reduced by the use, in the cathode feed vaporizer of the latest design, of a low permeability porous plug which is less sensitive to changes in pressure. However, this requires a higher operating temperature and more power. Consequently, a more satisfactory solution could ultimately result from the application

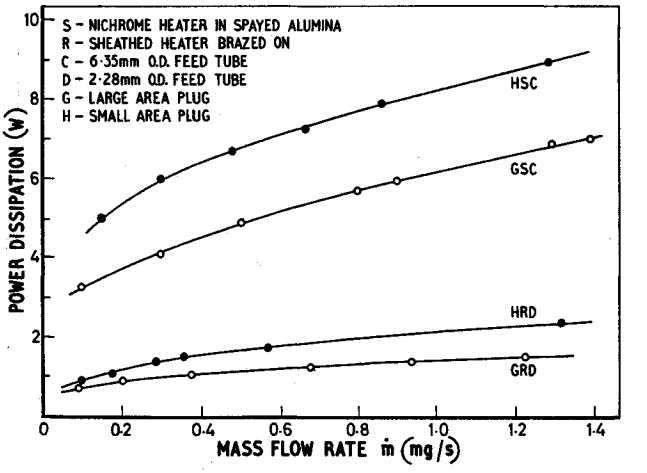

Fig. 11 Vaporizer power dissipation as a function of flow rate.

of a flow metering device, of the type described previously, to control the vaporizer temperature and maintain a constant value of $\dot{m}$.

A remaining problem concerns the long thermal time constant and inherent inaccuracies involved in taking flow rate measurements by the liquid phase technique. It was suggested in the previous section that this can be largely overcome by additional refinements to the vaporizer design, in particular by reducing the internal liquid volume and by providing adequate conductive cooling. It can be shown[2] that, for a vaporizer of tubular configuration with the dominant heat loss arranged to be conductive along the feed tube to a heat sink at its end, the approximate thermal time constant for cooling is proportional to the square of the feed tube length.

Consistency of Performance

In earlier tests,[2] it was shown that vaporizers constructed using porous tungsten plugs manufactured from material of the same nominal porosity yielded inconsistent flow rates, the variation being as great as $\pm 30\%$. While a part of this was attributed to fabrication problems, it has recently been shown that this scatter can be reduced to $\pm 7\%$ or less by a more controlled porous tungsten manufacturing process, and there is every hope of further improvement. In conjunction with the flow theory described below, this should lead to a more predictable vaporizer performance.

Flow Theory

The evaluation of fluid flow rates in porous media is never easy, but a theoretical relationship has been derived[2] which is in good agreement with practice. This was based on a simple model in which the flow takes place through a bundle of parallel capillaries and exhausts into a vacuum. Using the concept of flow conductance F, the theory was made applicable to both viscous and molecular flow regimes by introducing a factor Z[19] dependent on mean free path and capillary radius. For viscous flow $Z = 0.81$ and for molecular flow $Z = 1$. The resulting solution, using a tortuosity factor of $2^{1/2}$, is

$$F = Q/P = AP + B \quad \text{and} \quad \dot{m} = (PM/kT_A)(AP + B)$$

where

$$A = [f\pi R^2 a^2/32\eta l], \quad B = [6.79fkaT_A Z/(16)2^{1/2}\eta l](R/\sigma)^2$$

where f = fraction of mean cross section of porous plug open to flow, a = pore radius, k = Boltzman's constant, l = porous plug thickness, M = mass of mercury atom, Q = total volumetric flow rate at unit pressure, P = absolute pressure at porous plug inlet, R = porous plug radius, T_A = porous plug absolute temperature, η = gas or vapor viscosity at T_A, σ = effective molecular diameter.

The complementary experimental method[1,2] involved measuring the conductance of a vaporizer by observing the flow of a gas and, by plotting Q/P against P, allowed assessments of a and f to be made. These parameters were then used to calculate the mass flow rate of mercury vapor at various temperatures. As can be seen from Fig. 10, there was good agreement between vaporizer flow characteristics calculated on the above basis and experimental points obtained using mercury. The gas flow data indicated that the flow was normally in the transition regime, changing from free molecular to viscous as the applied pressure difference across the porous plug was increased from 10^5 to 10^6 dynes/cm^2 at 350°C.

Conclusions

The investigations reported here of the characteristics of tubular ceramic isolators have shown that steady-state breakdown voltages can be considerably increased by the insertion of porous insulating media. The minimum of the Paschen-type breakdown characteristic could be as high as 7.5 kv at 90 torr, with leakage currents below 10 μa, when using a 6-cm-long alumina tube tightly packed with small lead glass spheres. A manufacturing process has been established for reliably producing isolators of this type by sintering alumina spheres into a tube of the same material to form porous insulating cores.

It was shown, using an isolator integrated with a hollow cathode electron source operating under realistic discharge conditions, that the cathode plasma may be effectively screened by a plug of porous metal. It is proposed that charge recombination on internal surfaces and a nonuniform electric field distribution can explain the successful operation of these devices.

The isolator described here is thought to have a potentially superior performance and to have been brought to a higher stage of development than any previously reported for the same application, although extensive endurance testing has yet to be carried out.

A liquid mercury flowmeter giving a sensitivity of 0.8 mv $(\text{mg/sec})^{-1}$ with good linearity and reproducibility has been described. Comparison with theory shows that the device is capable of further development, leading to a substantially higher performance if required. In particular, independent studies[13] have shown that, by employing thermistors instead of thermojunctions as temperature sensing elements, increases in output voltage of several orders of magnitude should be possible with only minor modifications.

The use of a specially designed mercury vaporizer for controlling the mass flow rate through the flowmeter resulted in consistently high accuracy and a very short time constant for the stabilization of readings following flow rate adjustments. This was attributed to the small liquid capacity of the vaporizer.

A small efficient vaporizer has been designed which, in a number of forms, is capable of meeting the present requirement for three separate and independently controlled feeds to the ion thruster. A method of appreciably increasing the porous plug effective area, while maintaining the same overall vaporizer dimensions, has resulted in a significantly reduced power dissipation and working temperature for a given mass flow rate. Further refinements allowed a flow of 0.6 mg sec^{-1} to be achieved with a power of 1.2 w at 250°C. A theory has been developed which, when combined with a porous plug calibration technique, allows the performance of the vaporizer to be fairly accurately predicted.

References

[1] Fearn, D. G., Philip, C. M., and Pye, J. W., "The Development of Hollow Cathodes, Vaporizers and Isolators for Use in Mercury Ion Thrusters," *Proceedings of the Symposium Elektrische Antriebssysteme*, Deutsche Gesellschaft für Luft- und Raumfahrt, 71-22, 1971, pp. 61–83.

[2] Pye, J. W., "The Design and Development of Mercury Vaporizers for Use with Electron-Bombardment Ion Engines," TR 70042, 1970, Royal Aircraft Establishment, Farnborough, Hampshire, England.

[3] Day, B. P. and Hastings, R., "The RAE 10-cm Hollow-Cathode Ion Thruster," TR 71135, 1971, Royal Aircraft Establishment, Farnborough, Hampshire, England.

[4] Kerrisk, D. J. and Masek, T. D., "A Zero-Gravity Mercury Propellant Feed System," AIAA Paper 66-250, San Diego, Calif., 1966.

[5] Day, B. P. and Fearn, D. G., "A Review of Electric Propulsion Research in The United Kingdom," AIAA Paper 69-299, Williamsburg, Va., 1969; see also TR 69106, 1969, Royal Aircraft Establishment, Farnborough, Hampshire, England.

[6] Proctor, T. M. and Sutton, P. M., "Space-Charge Development in Glass," *Journal of the American Ceramic Society*, Vol. 43, No. 4, April 1960, pp. 173–179.

[7] Morse, C. T. and Hill, G. J., "The Effect of Porosity on the Electric Strength of Alumina," ERA 70-5, Feb. 1970, Electrical Research Association, Leatherhead, Surrey, England.

[8] Hackam, R., "Breakdown Potential of Mercury Vapor in Uniform Electric Fields," *International Journal of Electronics*, Vol. 28, No. 3, March 1970, pp. 263–269.

[9] Hackam, R., "Effects of Electrode Configuration and Voltage Polarity on the Electrical Breakdown of Mercury Vapor," *International Journal of Electronics*, Vol. 28, No. 1, Jan. 1970, pp. 79–87.

[10] Hackam, R., "Breakdown Potential of Mercury Vapor between Nickel Electrodes," *Journal of Physics*, Ser. D, Vol. 3, No. 11, Nov. 1970, pp. 1782–1784.

[11] Philip, C. M., "A Study of Hollow Cathode Discharge Characteristics," *AIAA Journal*, Vol. 9, No. 11, Nov. 1971, pp. 2191–2196.

[12] Donaldson, I. G., "Theoretical Considerations of a Micro Flowmeter," *Journal of Scientific Instruments*, Vol. 44, No. 12, Dec. 1967, pp. 1018–1022.

[13] Wilbur, P. J., "An Experimental Investigation of a Hollow Cathode Discharge," CR-120847, Dec. 1971, NASA.

[14] Pye, J. W. and Brabner, S., "Evaluation of a Liquid Mercury Flowmeter for Use with Ion Thrusters," Royal Aircraft Establishment, Farnborough, Hampshire, England, to be published.

[15] Kerslake, W. R., "Design and Test of Porous Tungsten Mercury Vaporizers," AIAA Paper 72–484, Bethesda, Md., 1972.

[16] Arlt, H. J., "A Propellant Feed System for Ion Thrusters," Proc. DGLR-*Proceedings of the Symposium Elektrische Antriebssysteme*, Deutsche Gesellschaft für Luft- und Raumfahrt, 71–21, June 1971, pp. 157–183.

[17] Rawlin, V. K. and Pawlik, E. V., "A Mercury Plasma-Bridge Neutralizer," AIAA Paper 67–670, Colorado Springs, Colo., 1967.

[18] Bessling, H., "Aufbau und Untersuchung eines Hg-Fördersystems für ein elektrostatisches Ionentriebwerk mit Autokathode," Rept. DLR Mitteilung 69–17, Aug. 1969.

[19] Dushman, Saul., *Scientific Foundations of Vacuum Techniques*, 2nd ed., Wiley, New York, 1962.